1 Investigation on the removal of the major cocaine metabolite (benzoylecgonine) in

2 water matrices by UV_{254}/H_2O_2 process by using a flow microcapillary film array

3 photoreactor as an efficient experimental tool.

4

5 Danilo Russo[a†], Danilo Spasiano[a], Marianna Vaccaro[a], Kristin H. Cochran[b], Susan D. Richardson[b],

6 Roberto Andreozzi[a], Gianluca Li Puma[c‡], Nuno M. Reis[c], Raffaele Marotta[a]

7

8 [a] Dipartimento di Ingegneria Chimica, dei Materiali e della Produzione Industriale, Università di

9 Napoli "Federico II", p.le V. Tecchio, 80 – 80125 – Napoli, Italy.

10 [b] Department of Chemistry and Biochemistry, University of South Carolina, Columbia, SC 29208,

11 USA.

12 [c] Environmental Nanocatalysis & Photoreaction Engineering Department of Chemical Engineering,

13 Loughborough University, Loughborough LE11 3TU, UK.

14

15 **Abstract**

16 A microcapillary film reactor (MCF) was adopted to evaluate and compare the removal efficiency

17 of benzoylecgonine (BE), an emerging micropollutant deriving from illicit drug abuse (cocaine), in

18 different aqueous matrices: milliQ water, synthetic and real wastewater and surface water. The

19 removal processes investigated were the direct photolysis with UV radiation at 254 nm, and the

20 advanced oxidative process (AOP) with the same UV radiation and hydrogen peroxide. As a result

21 of the microfluidics approach developed through an innovative experimental apparatus, full

22 conversion of BE was reached within a few seconds or minutes of residence time in the MCF

23 depending on the process conditions adopted. The radiation dose was estimated to be approximately

24 5.5 J cm^{-2}. The innovative MCF reactor was found to be an effective tool for photochemical studies,

25 especially when using highly priced, uncommon, or regulated substances. The removal efficiency

26   was affected by the nature of the aqueous matrix, due to the presence of different xenobiotics and

27   natural compounds that act primarily as $HO^{\bullet}$ radical scavengers and secondly as inner UV_{254} filters.

28   Moreover, nano-liquid chromatography (LC)-high resolution-mass spectrometry analysis was

29   utilized to identify the main reaction transformation products, showing the formation of

30   hydroxylated aromatics during the photochemical treatment.

31

32

33   [†] *Corresponding author.* Tel.: +39 081 7682253; fax: +39 081 5936936. E-mail address:

34   danilo.russo3@unina.it (D. Russo).

35   [‡] *Corresponding author.* Tel.: +44 (0)1509 222510; fax: +44 (0)1509 223923. E-mail address:

36   G.Lipuma@lboro.ac.uk (G. Li Puma).

37

40

1. Introduction

1.1. Benzoylecgonine as an emerging pollutant

43   In the last few decades, non-conventional micropollutant removal is an emerging research focus

44   (Asu et al., 2011; Corominas et al., 2013). The improvement in analytical technologies and the

45   increasing consumption of both illicit and legal drugs by the world population allowed the

46   discovery and identification in wastewater effluents (WW) and surface water (SurW) of new classes

47   of contaminants, such as pharmaceuticals (Zuccato et al., 2009) and personal care products (Huerta-

48   Fontela et al., 2008a; Bartelt-Hunt et al., 2009). Among these contaminants of emerging concern, in

49   the last few years, the scientific literature shows an increasing interest in substances deriving from

50   illicit drug consumption (Richardson et al., 2014; Richardson, 2012). These compounds reach

51   wastewater treatment plants (WWTPs) through the drug users' urine and faeces and then are

52 released into the environment unchanged or as metabolites (Zuccato et al., 2009; Castiglioni et al.,

53 2008). The eco-toxicological effects for most of these compounds are unknown, but their potential

54 hazard cannot be excluded (Huerta-Fontela et al., 2008b; Kasprzyk-Hordern et al., 2008; Repice et

55 al., 2008). Cannabinoids, cocaine, opiates, and amphetamine-like drugs are the most used illicit

56 drugs worldwide (van Nuijs et al., 2011). Cocaine is the second most used illicit drug in Europe

57 (World Drug Report, 2012). In the human body, only 1-9% of consumed cocaine is excreted in

58 urine as the unchanged parent drug, whereas the rest of it is metabolized to benzoylecgonine (45%)

59 and ecgonine methyl ester (40%) (Castiglioni et al., 2008). Consequently, benzoylecgonine (Fig. 1)

60 is the primary metabolite of cocaine, and it was found in almost all the WW and SurW samples in

61 Europe and in other parts of the world at higher levels than its parent compound (Irvine et al., 2011;

62 Yin Lai et al., 2013).

63 Moreover, while cocaine and its metabolite ecgonine methyl ester tend to spontaneously degrade in

64 WW and SurW effluents (more or less rapidly depending on the pH and temperature),

65 benzoylecgonine (BE) concentration is almost constant or slightly increasing, due to its relative

66 stability in aqueous matrices and the partial degradation of cocaine into BE (Castiglioni et al., 2006;

67 Gheorghe et al., 2008; Castiglioni et al., 2011; van Nuijs et al., 2012). Tables S1 a-b in the

68 supplementary information section show the BE levels reported in SurW and WWTPs effluents.

69 The finding of BE in WWTPs effluents attests to the incomplete removal in conventional plants.

70 Because of its relatively high levels in the inlet, even with good removal efficiency ($\geq$ 80%), the

71 levels in the effluents are still higher than other illicit drug contaminants (Huerta-Fontela et al.,

72 2008; Kasprzyk-Hordern et al., 2008; Postigo et al., 2009; Repice et al., 2013; Du et al., 2014).

73 Despite the presence of illicit drug contaminants in WW and SurW, there are only a few studies

74 addressing the eco-toxicological effects of BE on the aquatic environment. The exposure of

75 *Dreissena polymorpha* (a zebra mussel) to BE concentrations of 0.5 and 1.0 µg $\cdot$L^{-1}, resulted in a

76 3.5 fold increase of the oxidative stress in comparison to the background level and either an

77 increased or inhibited activity of antioxidant and detoxifying enzymes depending on the BE levels

78 and the exposure time (Parolini et al., 2013). In addition, an increased peroxidation of lipids and

79 protein carbonylation, DNA damage, and cellular apoptotic death were found in experiments carried

80 out up to 14 days (Binelli et al., 2013). Even more detrimental damage cannot be excluded at

81 longer exposure times and in concert with the effects of other WW and SurW micropollutants.

82 The kinetic behaviour of BE during a disinfection stage for water reuse was previously investigated

83 (Russo et al., 2016) treating contaminated milliQ water under UV_{254} radiation only.

84 The purpose of this study is to investigate the effect of an advanced oxidation process (AOP) with

85 hydrogen peroxide and UV_{254} radiation on the removal and transformation of BE in four different

86 aqueous matrices: milliQ water, synthetic wastewater (SWW), real wastewater (RWW) and SurW.

87 *1.2. Microcapillary photoreactor*

88 The degradation experiments were carried out in a novel microcapillary film (MCF) array photo-

89 reactor (Reis and Li Puma, 2015) consisting of 10 microcapillaries with a mean diameter of about

90 200 μm transparent to UVC light. A schematic of the reactor is reported in fig. S1 in the

91 supplementary information section. This experimental apparatus allows the use of very small

92 volumes of reacting solution compared to the usual batch photo-reactors, leading to economic and

93 environmental benefits. A significant benefit is the reduction of the volume of the experimental

94 waste solution and decreased usage of costly border controlled substances, including the adoption of

95 illicit drugs as the tested compounds. The cost of the low power (8 W) UV lamp necessary for this

96 kind of reactor is also very low. Moreover, as described elsewhere (Reis and Li Puma, 2015; Russo

97 et al., 2016), the extremely small reactor volume and optical path length allows for complete

98 conversion of the contaminant in a few seconds or a few minutes depending on the treatment

99 adopted. This is possible as a result of the high surface/volume ratio achievable in a microcapillary

100 reactor and high photon irradiance, which is realized even in optically thick fluids. Therefore, the

101 MCF photoreactor represents a powerful tool for the rapid determination of photodegradation

102 kinetics of contaminants in fluids at a laboratory scale. The wider impact of this study will be

103 maximized by the integration of MCF with ultra-rapid analytics for the determination of

4

104   transformation products of contaminants of emerging concern which are often available only in

105   minute quantities.

106

107   **2. Materials and methods**

108   *2.1. Materials*

109   Hydrogen peroxide (30% v/v), benzoylecgonine ($\geq$ 99% w/w), acetonitrile ($\geq$ 99.9% v/v), formic

110   acid ($\geq$ 95% v/v), sodium hydroxide, and sulfuric acid were purchased from Sigma-Aldrich. The

111   milli-Q water was prepared by a Millipore Elix water purification system.

112   Synthetic wastewater was prepared following the OECD Guidelines (Organisation for Economic

113   Cooperation and Development, 1999) using milliQ water and peptone (32 ppm), meat extract (22

114   ppm), urea (6 ppm), K_2HPO_4 (28 ppm), $CaCl_2 \cdot H_2O$ (4 ppm), NaCl (7 ppm) and Mg_2SO_4 (0.6 ppm).

115   These substances were purchased from Sigma-Aldrich. Real wastewater was sampled from the

116   sewage water treatment plant of Festival Drive, Loughborough, Leichestershire (UK). Surface water

117   was collected from the Grand Union Canal in the same zone. All the real water samples were

118   filtered through Whatman nylon filters (0.45 μm), to avoid clogging of the MCF and of the high

119   performance liquid chromatography (HPLC) tubing. Furthermore, this allowed the direct evaluation

120   of the degradation of BE in the different aqueous matrices without considering the effect of the

121   suspended solid matter on the absorption of radiation and sorption of BE and its transformation

122   products (TPs).

123   *2.2. Analytical methods*

124   The concentrations of hydrogen peroxide and BE in the samples were evaluated by HPLC analysis.

125   The HPLC (1100 Agilent) apparatus was equipped with a Gemini C18 (Phenomenex) reverse phase

126   column and a diode array UV/VIS detector (λ = 232 nm). The mobile phase consisted of a mixture

127   of formic acid aqueous solution (25 mM) (A) and acetonitrile (B) flowing at 0.6 mL min^{-1}. The

128   following gradient was adopted: 7% B to 28% B in 9 min, to 50% B in 5 min, constant for 2 min,

129   and then to 35.7% in 3 min, and finally returned to the initial conditions in 5 min. The retention

130   times of H_2O_2 and BE were 4.9 min and 13.8 min, respectively. The pH of the reacting solutions

131   was measured with an Accumet Basic AB-10 pH-meter. A Perkin Elmer UV/VIS spectrometer

132   (Lambda 35) was used to determine the absorbance spectra of the aqueous matrices. The

133   conductivity and the total organic carbon (TOC) of the water samples were respectively measured

134   with a WPA Linton Cambridge CM35 conductivity meter and a TOC-5000A TOC analyzer

135   (Shimadzu). The nitrate and nitrite content were measured by means of ion chromatography

136   (Metrohm 761 Compact). Table 1 summarizes the main water features.

137   *2.3. Experimental apparatus and procedures*

138   *2.3.1. Apparatus and treatment*

139   The spiked solutions were prepared by adding the solid BE to each filtered aqueous matrix. The

140   initial concentration of BE in the solutions was kept in the range $2.8 \cdot 10^{-5} \pm 4.0 \cdot 10^{-6}$ mol L^{-1}. This

141   value is much greater than the usual level of BE found in RWW and SurW (Tab. S1); however, it

142   was necessary to keep the concentration at a higher level for a better evaluation and comparison of

143   the removal kinetics and for the identification of the transformation byproducts.

144   In order to study the degradation of BE with the UV_{254}/H_2O_2 process, a fluorinated ethylene-

145   propylene (FEP-Teflon) MCF photoreactor containing 10 capillaries with a mean hydraulic

146   diameter of 195 μm was used. The description and the validation of the microreactor has been

147   described in detail elsewhere (Reis and Li Puma, 2015; Russo et al., 2016). As previously reported,

148   the microreactor was coiled around a 8 W (nominal power) UV monochromatic lamp (Germicidal

149   G8T5) emitting radiation at 254 nm. The segments not coiled were covered with aluminum foil to

150   avoid UV radiation reaching these sections. Experiments were performed in continuous flow

151   through the reactor. The residence time (i.e., the reaction time) was changed by varying the length

152   of the reactor exposed to the UV_{254} radiation. Samples at different residence times were collected

153   from the outlet of the MCF after reaching the steady state condition (i.e., about 5 times the reactor

154   volume processed) and rapidly analyzed. The concentration of BE in the inlet to the reactor did not

155   vary during the experimental runs. All experiments were carried out at room temperature (~ 25 °C).

156 It was verified that thermostatic control was not necessary because at the outlet of the reactor, the

157 temperature of the solution did not vary significantly. The pH of the reacting solutions was adjusted

158 with dilute solutions of NaOH and H_2SO_4. At the end of each experiment, the pH of the solutions

159 was re-measured and the results were always close to the initial value.

160 *2.3.2. Analysis of transformation products*

161 Aqueous reaction mixtures and untreated controls were extracted using solid phase extraction (SPE)

162 and analyzed using LC-mass spectrometry (MS)/MS. Water samples (150 mL) were passed through

163 SPE cartridges (Waters Oasis HLB, 6cc) at a rate of approximately 5 mL/min and were eluted with

164 8 mL of methanol, in 4 mL increments, using gravity elution. The eluted solutions were stored in

165 the freezer throughout the duration of the experiments. They were either used as is or blown down

166 using nitrogen to make a more concentrated solution.

167 Mass spectrometry analyses of TPs were carried out using a high resolution Thermo Orbitrap Velos

168 Pro (Thermo Scientific, Bremen, Germany). A nano-LC was coupled to the Orbitrap for

169 chromatographic separation. The flow rate was 0.300 μL/min. Initial conditions were 2% organic

170 (acetonitrile) and were held for 5 min. The percent organic was ramped linearly to 40% over the

171 next 10 min, then ramped linearly to 95% over the next 40 min, held at 95% for 10 min, and then

172 returned to initial conditions. The capillary voltage was 1.8 kV. The column used was a picochip

173 C18 reversed phase column (10 cm x 75 μm; 3 μm; New Objective; Woburn, MA). The injection

174 volume was 1 μL and the column temperature was held at room temperature. Full-scan and data-

175 dependent acquisition (DDA) MS/MS spectra were obtained using positive ion electrospray

176 ionization (ESI). The resolution was 30,000 for full-scan MS, and 7500 for DDA. The mass range

177 was *m/z* 100-800.

178 A fraction containing two transformation product isomers (TP305) was also collected via

179 continuous fractionation with preparative LC-MS using a Waters 2000 series LC-mass spectrometer

180 with a C18 column and single quadrupole detector. An acetonitrile/water gradient was used, with a

181 100 μL injection volume and 1.0 mL/min flow rate. The fractions were collected based on retention

182   times. After collection, the sample was freeze dried and dissolved in deuterated methanol (d4) and

183   analyzed using ^{1}H nuclear magnetic resonance (NMR) with a Bruker Avance III-HD 400 MHz

184   NMR spectrometer.

185   In this study, TPs are named using a number referring to their molecular mass (e.g., TP 305 refers to

186   a TP with a molecular mass of 305 Da).

187

188   **3. Results and Discussion**

189   *3.1. Degradation Absorbance Characteristics*

190   Absorbance spectra were acquired to characterize and compare the different aqueous matrices. Fig.

191   2a. shows the characteristic absorption peak of BE in milliQ water at the wavelength of 232 nm. No

192   significant differences were observed in the spectra in the pH range 4-8. This was confirmed by the

193   mean reported values of pK_{a1} and pK_{a2} of BE, that are 3.35 and 10.45, respectively (Jeanville et al.,

194   2003; Marchi et al., 2009). The spectra of filtered SWW, RWW, and SurW are also displayed in

195   Fig. 2b. The absorbances were nearly coincident for the real wastewater and surface water samples,

196   whereas the synthetic wastewater showed very low absorbance at 254 nm. This can be ascribed to

197   the higher concentration of the aromatic compounds dissolved in the real wastewater and surface

198   water samples compared to the lower concentrations of these in the synthetic wastewater, which is

199   also supported by the TOC data in Table 1. This difference does not significantly affect the BE

200   removal, as further discussed, because of the different nature of the organic compounds.

201   Control experiments performed in pH range 4-8 with direct photolysis and with the UV_{254}/H_2O_2

202   process showed insignificant differences in the removal of BE (data not shown).Consequently, all

203   further experiments were run at pH = 6.0 in milliQ water and at natural pH for the other different

204   aqueous matrices (Table 1). Moreover, no BE degradation was recorded in the presence of

205   hydrogen peroxide ($[H_2O_2]/[BE] \sim 500$) without UV_{254} radiation (data not shown).
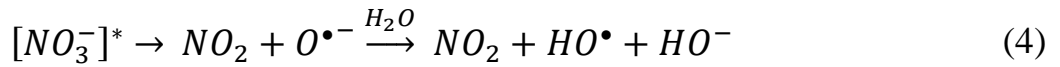
206   *3.2. Degradation Kinetics*

207   Figure 3 shows the removal percentage of BE by direct UV_{254} photolysis at different residence

208   times in the MCF and with the different aqueous matrices that were examined, compared to

209   previously published removal in milliQ water. Even though UV treatment is not often adequate for

210   chemical removal, it is important to consider that in the case of water reuse, UV treatment is

211   indicated as a method to reduce the presence of pathogens. During this process a contemporary

212   transformation of chemicals cannot be excluded.

213   The removal rate of BE in the SWW sample was slower than in milliQ water. This rate difference

214   could be ~~easily~~ justified by the presence of several compounds in SWW that may act as inner filters

215   (optical competitors absorbing part of the radiation) since the absorption of the SWW at 254 nm

216   (Fig. 2) was slightly higher than the absorbance of milliQ represented by the zero line in the

217   absorbance spectrum. In spite of this, as reported elsewhere (De Laurentiis et al., 2012), while the

218   chromophoric dissolved organic matter would inhibit the direct photolysis of BE by an inner-filter

219   effect, it could simultaneously act as a producer of oxidant species that could promote BE

220   degradation. Therefore, the degradation of BE showed in fig. 2 must be considered as a result of the

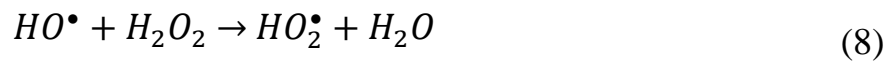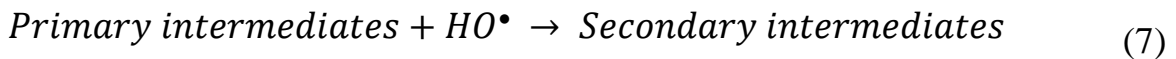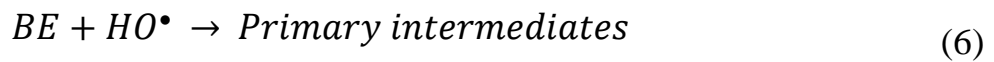221   balance of the effects described above.

222   Moreover, the BE removal percentage and rate in SurW is very close to the removal in milliQ

223   water, whereas in RWW effluents is significantly faster. These phenomena occur despite both SurW

224   and RWW samples having considerably greater absorbances than the milliQ water. This evidence

225   could suggest that the inner filter effect from the dissolved species was fully or more than offset by

226   the chemical nature of the organic compounds present in these water matrices. Specifically, the

227   photolysis of nitrates are a supplementary source of hydroxyl radicals (Mack and Bolton, 1999) and

228   since the nitrate content of the RWW sample was double that of the SurW sample, (Table 2), the

229   removal of BE in the RWW water matrix could be expected to be higher than in the SurW sample

230   (Fig. 3). This effect has also been reported for the removal of other water contaminants (Alif and

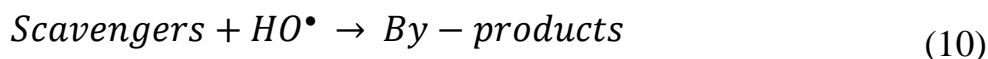231   Boule, 1991; Pamela et al., 1998; Goldstein and Rabani, 2008; Keen et al., 2012; Ji et al., 2012; Li

et al., 2014; Zaviska et al., 2014). The nitrate photolysis follows the pathways below (Mack and Bolton, 1999):

$$NO_3^- \xrightarrow{h\nu} NO_2^- + \frac{1}{2} O_2 \tag{1}$$

$$NO_3^- \xrightarrow{h\nu} [NO_3^-]^* \tag{2}$$

$$[NO_3^-]^* \rightarrow NO_2^- + O(^3P) \tag{3}$$

$$[NO_3^-]^* \rightarrow NO_2 + O^{\bullet -} \xrightarrow{H_2O} NO_2 + HO^\bullet + HO^- \tag{4}$$

$HO^\bullet$ radicals increase the removal rate of BE in the RWW sample by oxidizing the organic contaminant (Fig. 3). The possibility that the photolysis of nitrite could contribute to the generation of hydroxyl radicals is not considered because of their negligible content compared to nitrates concentration (Tab. 1).

 Once the effects of different aqueous matrices on the indirect photolysis of BE were investigated, the removal of BE by UV_{254}/H_2O_2 process was studied. The photolysis of the H_2O_2 molecule, with radiation at 254 nm, yields two strongly reactive $HO^\bullet$ radicals. The reaction pathways can be exemplified as follow:

$$H_2O_2 \xrightarrow{h\nu} 2HO^\bullet \tag{5}$$

$$BE + HO^\bullet \rightarrow Primary\ intermediates \tag{6}$$

$$Primary\ intermediates + HO^\bullet \rightarrow Secondary\ intermediates \tag{7}$$

$$HO^\bullet + H_2O_2 \rightarrow HO_2^\bullet + H_2O \tag{8}$$

$$2HO_2^\bullet \rightarrow H_2O_2 + O_2 \tag{9}$$

$$Scavengers + HO^\bullet \rightarrow By-products \qquad (10)$$

242   Reaction (10) describes the scavenging effect of the organic compounds naturally or artificially

243   present in the water. This reaction was not considered for the process in milliQ water due to the

244   absence of organic contaminants. However, $HO^\bullet$ radical production via reactions 1-4 was

245   considered where necessary. Mack and Bolton (1999) report that, using UV and nitrate, hydroxyl

246   radical generation is not as efficient as the $HO^\bullet$ production with hydrogen peroxide. The reduced

247   UV/nitrate efficiency is due to the nitrate's low hydroxyl radical quantum yield in the 250 nm to

248   350 nm range compared to the quantum yield of direct photolysis of hydrogen peroxide $\Phi_{254}^{H_2O_2} =$

249   0.5 mol ein^{-1} (Nicole et al., 1990). Consequently reaction (5) is faster than (4) in the presence of

250   nitrates in the water.

251   Fig. 4 displays the effect of different $[H_2O_2]_o/[BE]_o$ ratios on the removal efficiency in milliQ water,

252   where $[H_2O_2]_o$ and $[BE]_o$ are respectively the initial concentrations of hydrogen peroxide and BE.

253   Higher $[H_2O_2]_o/[BE]_o$ ratios resulted in greater percentages of removal. Fig. 5 shows the BE

254   percentage of removal at different $[H_2O_2]_o/[BE]_o$ ratios for the four types of water matrices at three

255   significant reaction times.

256   However, the gain in the removal percentage gradually lessens with increased $[H_2O_2]_o/[BE]_o$ ratio,

257   such that the removal degree at a fixed reaction time reached a plateau for all aqueous matrices

258   investigated (Fig. 5). In effect, an increase of the relative hydrogen peroxide concentration results

259   also in increased rate of reaction (8) so that a smaller than expected amount of hydroxyl radicals is

260   effective in the degradation. The high $[H_2O_2]_o/[BE]_o$ ratios adopted in this experiment can be

261   justified because in real wastewater samples collected worldwide, BE is just one of many

262   micropollutants found in effluents and in surface waters. A greater hydrogen peroxide concentration

263   may be necessary for efficient degradation of these different mixtures of xenobiotics normally

264   present in water bodies.

265 A comparison of the time scale of UV_{254} direct photolysis against UV_{254}/H_2O_2 removal of BE

266 shows significantly different characteristic kinetics of the two processes. The UV_{254} radiation

267 treatment (Fig. 3) requires up to two orders of magnitude longer time for the degradation of BE

268 compared to the UV_{254}/H_2O_2 process (Fig. 4). The difference in magnitude suggests that direct

269 photolysis is a negligible process during the AOPs and that it would be highly inefficient on its own

270 for BE degradation.

271 As shown in Fig. 5, BE removal is higher in milliQ water once all of the operating conditions are

272 standardized between the different aqueous matrices. This phenomenon is due to the absence of

273 organic molecules acting as scavengers of hydroxyl radicals. However, the presence of scavengers

274 alone cannot justify the differences in rates between RWW effluent and natural SurW. The rate

275 differences can be related to the balance between the contrasting effects of reactions 1-4. In almost

276 all of the experiments, the removal percentages in RWW samples are slightly but significantly

277 higher than in SurW. Similarly to what was reported for direct photolysis, this last evidence is in

278 agreement with RWW having a higher nitrate concentration with respect to SurW since the

279 absorbance of the two aqueous matrices is comparable (Fig 2).

280 *3.3. Transformation Products*

281 Several transformation products (TPs) resulting from UV photolysis and UV/H_2O_2 treatment of BE

282 were observed. These products increased in abundance with increasing reaction time, and they were

283 tentatively identified using their accurate masses (Orbitrap-MS) and MS/MS fragmentation. Fig. 6

284 shows some of the most prominent TPs found in UV/H_2O_2 reactions of BE, in which 40% of BE

285 was degraded (~ 0.5 s reaction time). These products were also present at 90% and 100%

286 degradation of BE, as well as in samples treated with UV only.

287 Three of these TPs (TP 305a, 305b, and 305c, fig. 6a) appear to be isomers, each having an

288 observed accurate mass of *m/z* 306.1348 (as the (M+H)$^+$ ion), and eluting at 20.56, 21.18, and 23.05

289 min, respectively. Their accurate mass suggests a molecular formula of $C_{16}H_{19}NO_5$ (theoretical

290 mass of *m/z* of 306.1336). These TPs are likely monohydroxylated isomers, meta-, para-, and ortho-

12

291   hydroxybenzoylecgonine. The MS/MS product ion spectra support these structural assignments. At

292   a CE of 40 eV, two distinct fragments (*m/z* 168.1023 and 121.0287, fig. 7) matched viable

293   fragmentation on the two bonds on either side of the ester oxygen (theoretical *m/z* of 168.1024 and

294   121.0289, respectively, for these two fragment ions). In particular, the *m/z* 121.0287 fragment ion,

295   with a formula of $C_7H_5O_2$, indicates that hydroxyl radical addition occurs on the benzene ring,

296   which is consistent with UV and UV/H_2O_2 chemistry (Andreozzi et al., 2003).

297   Two of these TPs were isolated using preparative LC-MS, and NMR data supported the assignment

298   of the ortho- and para-hydroxylated TPs. Despite low levels collected from these reaction mixtures,

299   there was strong evidence for the ortho-hydroxy-BE [H6 d (J = 5.5 Hz), δ = 8.208 ppm; H4 m, δ =

300   7.740 ppm; H3 d (J = 8.04 Hz), δ = 7.630 ppm; H5 t (J = 8.04 Hz), δ = 7.478 ppm]. The para-

301   hydroxy-BE assignment was also suggested by NMR data [H2,6 broad singlet, δ = 7.831 ppm; H3,5

302   broad singlet δ = 7.207 ppm], but it was not as definitive, due to lower levels of this TP isolated

303   relative to the ortho isomer. These TPs were also reported as by-products formed during two solar

304   photocatalytic treatments (TiO$_2$ photocatalysis and photo-Fenton) of cocaine in water (Postigo et al.

305   2011).

306   TP 321 was observed at *m/z* 322.1300 ((M+H)$^+$ ion). This TP is likely dihydroxybenzoylecgonine,

307   which has a theoretical *m/z* of 322.1285 for the (M+H)$^+$ ion. This TP eluted at 19.36, 21.84 min, and

308   25.12 min, and likely has both hydroxyl substituents on the benzene ring, consistent with TP 305a,

309   305b, and 305c, and consistent with hydroxyl radical chemistry. It is currently not known which

310   isomer this TP represents (6 isomers are possible). MS/MS data provide evidence that the three

311   chromatographic peaks in Fig. 6B indicate three isomers of dihydroxybenzoylecgonine, all of which

312   have the two hydroxyl substituents on the aromatic ring. When the TP was fragmented using CID

313   (27 eV), the resulting fragmentation pattern matches the half of the parent molecule with the

314   bridged ring and no evidence of the hydroxyl groups. The half with the aromatic ring (and hydroxyl

315   groups) breaks off as a neutral molecule and is not observed by the detector. Three chromatographic

316   peaks for TP 321 were seen in the MS/MS data, and all of them yielded the same fragmentation

13

317   pattern as discussed above. Work continues to identify other less predominant TPs, as well as to

318   collect additional individual TP fractions (using preparative-LC-MS) for nuclear magnetic

319   resonance (NMR) analysis and confirmation of proposed chemical structures. NMR is particularly

320   helpful for determining substituent positions, and can aid in the identification of specific isomers for

321   TPs for cases where MS spectra are not definitive (Wendel et al., 2014; Luft et al., 2014). Further

322   chemical characterization of transformation products will be done using 2-dimensional NMR

323   spectroscopy on transformation products isolated with preparative-LC, and further mass

324   spectrometry analyses will be performed using targeted MS/MS on selected degradation products.

325

326

327   **4. Conclusions**

328   • The microfluidics approach adopted in this study allowed a full investigation on the removal of

329   benzoylecgonine by photolysis and the UV_{254}/H_2O_2 process using minute quantities (100 mg) of

330   this border controlled substance.

331   • Benzoylecgonine, the primary human urinary metabolite of cocaine, was efficiently removed by

332   UV_{254} photolysis coupled with H_2O_2 in a microcapillary film photoreactor at approximately neutral

333   pH. The removal efficiency was affected by the nature of the aqueous matrix.

334   • Mass spectrometry analyses showed a significant decrease of benzoylecgonine and subsequent

335   increase in transformation products. The potential toxicity of these compounds is as yet unknown.

336

340

341   **References**

342 Alif, A., Boule, P., 1991. Photochemistry and environment part XIV. Phototransformation of

343 nitrophenols induced by excitation of nitrite and nitrate ions. J. Photochem. Photobiol. A: Chem.

344 59, 357–367.

345 Andreozzi, R., Caprio, V., Marotta, R., Vogna, D., 2003. Paracetamol oxidation from aqueous

346 solutions by means of ozonation and H_2O_2/UV system. Water Research 37, 993–1004.

347 Asu, Z., Nilsun, H.I., 2011. The occurrence and fate of anti-inflammatory and analgesic

348 pharmaceuticals in sewage and fresh water: Treatability by conventional and non-conventional

349 processes. Journal of Hazardous Materials 187, 24–36.

350 Bartelt-Hunt, S.L., Snow, D.D., Damon, T., Shockley, J., Hoagland, K., 2009. The occurrence of

351 illicit and therapeutic pharmaceuticals in wastewater effluent and surface waters in Nebraska.

352 Environmental Pollution 157, 786–791.

353 Berset, J.D., Brenneisen, R., Mathieu, C., 2010. Analysis of licit and illicit drugs in waste, surface

354 and lake water samples using large volume direct injection high performance liquid

355 chromatography – electrospray tandem mass spectrometry (HPLC-MS/MS). Chemosphere 81, 859–

356 866.

357 Bijlsma, L., Emke, E., Hernandez, F., de Voogt, P., 2012. Investigation of drugs of abuse and

358 relevant metabolites in Dutch sewage water by liquid chromatography couples to high resolution

359 mass spectrometry. Chemosphere 89, 1399–1406.

360 Binelli, A., Marisa, I., Fedorova, M., Hoffmann, R., Riva, C., 2013. First evidence of protein profile

361 alteration due to main cocaine metabolite (benzoylecgonine) in a freshwater biological model.

362 Aquatic Toxicology 140-141, 268–278.

363 Bones, J., Thomas, K.V., Brett, P., 2007. Using environmental analytical data to estimate levels of

364 community consumption of illicit drugs and abused pharmaceuticals. Journal of Environmental

365 Monitoring 9, 701–707.

15

366   Castiglioni, S., Zuccato, E., Crisci, E., Chiarabrando, C., Fanelli, R., Bagnati, R., 2006.

367   Identification and measurements of illicit drugs and their metabolites in urban wastewater by liquid

368   chromatography-tandem mass spectrometry. Analytical Chemistry 78(24), 8421–8429.

369   Castiglioni, S., Zuccato, E., Chiarabrando, C., Fanelli, R., Bagnati, R., 2008. Mass spectrometric

370   analysis of illicit drugs in wastewater and surface water. Mass Spectrometry Reviews 27, 378–394.

371   Castiglioni, S., Bagnati, R., Melis, M., Panawennage, D., Chiarelli, P., Fanelli, R., Zuccato, E.,

372   2011. Identification of cocaine and its metabolites in urban wastewater and comparison with human

373   excretion profile in urine. Water Research 45, 5141–5150.

374   Corominas, L., Foley, J., Guest, J.S., Hospido, A., Larsen, H.F., Morera, S., Shaw, A., 2013. Life

375   cycle assessment applied to wastewater treatment: State of the art. Water Research 47, 5480−5492.

376   De Laurentiis, E., Chiron, S., Kouras-Hadef, S., Richard, C., Minella, M., Maurino, V., Minero, C.,

377   Vione, D., 2012. Photochemical fate of carbamazepine in surface freshwaters: laboratory measures

378   and modelling. Environmental Science & Technology 46, 8164-8173.

379   Du, B., Price, A.E., Scott, W.C., Kristofco, L.A., Ramirez, A.J., Chambliss, C.K., Yelderman, J.C.,

380   Brooks, B.W., 2014. Comparison of contaminants of emerging concern removal, discharge, and

381   water quality hazards among centralized and on-site wastewater treatment system effluents

382   receiving common wastewater influent. Science of Total Environment 466-467, 976-984.

383   Gheorghe, A., Van Nuijs, A., Pecceu, B., Bervoets, L., Jorens, P.G., Blust, R., Neels, H., Covaci,

384   A., 2008. Analysis of cocaine and its principal metabolites in waste and surface water using solid-

385   phase extraction and liquid chromatography-ion trap tandem mass spectrometry. Anal. Bioanal.

386   Chem. 391, 1309-1319.

387   Goldstein, A., Rabani, J., 2008. Polychromatic UV photon irradiance measurements using chemical

388   actinometers based on NO_3^- and H_2O_2 excitation: applications for industrial photoreactors.

389   Environmental Science & Technology 42, 3248-3253.

390   Huerta-Fontela, M., Galceran, M.T., Ventura, F., 2007. Ultraperformance liquid chromatograph-

391   tandem mass spectrometry analysis of stimulatory drugs of abuse in wastewater and surface waters.

392   Analytical Chemistry 79, 3821-3829.

393   Huerta-fontela, M., Galceran, M.T., Ventura, F., 2008a. Stimulatory drugs of abuse in surface

394   waters and their removal in a conventional drinking water treatment plant. Environmental Science

395   & Technology 42, 18.

396   Huerta-Fontela, M., Galceran, M.T., Martin-Alonso, J., Ventura, F., 2008b. Occurrence of

397   psychoactive stimulatory drugs in wastewaters in noth-eastern Spain. Science of the Total

398   Environment 397, 31-40.

399   Hummel, D., Loeffler, D., Fink, G., Ternes, T.A., 2006. Simultaneous determination of

400   psychoactive drugs and their metabolites in aqueous matrices by liquid chromatography mass

401   spectrometry. Environmental Science and Technology 40, 7321-7328.

402   Irvine, R.J., Kostakis, C., Felgate, P.D., Jaehne, E.J., Chen, C., White, J.M., 2011. Population drug

403   use in Australia: a wastewater analysis. Forensic Science International 210, 69-73.

404   Jeanville, P. M., Estapé, E.S., Torres-Negròn de Jeanville, I., 2003. The effect of liquid

405   chromatography eluents and additives on the positive ion responses of cocaine, benzoylecgonine,

406   and ecgonine methyl ester using electrospray ionization. International Journal of Mass Spectrometry

407   227, 247-258.

408   Ji, Y., Zeng, C., Ferronato, C., Chovelon, J., Yang, X., 2012. Nitrate-induced photodegradation of

409   atenolol in aqueous solution: kinetics, toxicity and degradation pathways. Chemosphere 88, 644-

410   649.

411   Karolak, S., Nefau, T., Bailly, E., Solgadi, A., Levi, Y., 2010. Estimation of illicit drugs

412   consumption by wastewater analysis in Paris area (France). Forensic Science International 200,

413   153-160.

414   Kasprzyk-Hordern, B., Dinsdale, R.M., Guwy, A.J., 2008. The occurrence of pharmaceuticals,

415   personal care products, endocrine disruptor and illicit drugs in surface water in South Wales, UK.

416   Water Research 42, 3498-3518.

417   Kasprzyk-Hordern, B., Dinsdale, R.M., Guwy, A.J., 2009. The removal of pharmaceuticals,

418   personal care products, endocrine disruptors and illicit drugs during wastewater treatment and its

419   impact on the quality of receiving waters. Water Research 43, 363-380.

420   Keen, O.S., Love, N.G., Linden, K.G., 2012. The role of effluent nitrate in trace organic chemical

421   oxidation during UV disinfection. Water Research 46, 5224-5234.

422   Li, Y., Niu, J., Shang, E., Zheng, M., Luan, T., 2014. Effects of nitrate and humic acid on

423   enrofloxacin photolysis in an aqueous system under three light conditions: kinetics and mechanism.

424   Environmental Chemistry 11(3), 333-340.

425   Luft, A., Wagner, M., Ternes, T.A., 2014. Transformation of Biocides Irgarol and Terbutryn in the

426   Biological Wastewater Treatment. Environmental Science & Technology 48, 244−254.

427   Mack, J., Bolton, J.R., 1999. Photochemistry of nitrite and nitrate in aqueous solution: a review.

428   Journal of Photochemistry and Photobiology A 128, 1−13.

429   Marchi, I., Rudaz, S., Veuthey, J., 2009. Sample preparation development and matrix effects

430   evaluation for multianalyte determination in urine. Journal of Pharmaceutical and Biomedical

431   Analysis 49, 459-467.

432   Mari, F., Politi, L., Biggeri, A., Accetta, G., Trignano, C., Di Pauda, M., Bertol, E., 2009. Cocaine

433   and heroin in waste water plants: a 1-year study in the city of Florence, Italy. Forensic Science

434   International 189, 88-92.

435   Mendoza, A., Lopez de Alda, M., Gonzalez-Alonso, S., Mastroianni, N., Barcelò, D., Valcarcel, Y.,

436   2014. Occurrence of drugs of abuse and benzodiazepines in river waters from the Madrid Region

437   (Central Spain). Chemosphere 95, 247-255.

438   Metcalfe, C., Tindale, K., Li, H., Rodayan, A., Yargeau, V., 2010. Illicit drugs in Canadian

439   municipal wastewater and estimates of community drug use. Environmental Pollution 158, 3179-

440   3185.

441   Nicole, I., De Laat, J., Doré, M., Duguet, J.P., Bonnel, C., 1990. Use of UV radiation in water

442   treatment: measurement of photonic flux by hydrogen peroxide actinometry. Water Research 24,

443   157-168.

444   Organisation for Economic Cooperation and development (OECD), 1999. Guidelines for testing of

445   Chemicals, Simulation Test-Aerobic Sewage Treatment. 303A.

446   Pamela, P., Vaughan and Neil V. Blough, 1998. Photochemical formation of hydroxyl radical by

447   constituents of natural waters. Environmental Science & Technology 32, 2947-2953.

448   Parolini, M., Pedriali, A., Riva, C., Binelli, A., 2013. Sub-lethal effects caused by the cocaine

449   metabolite benzoylecgonine to the freshwater mussel Dreissena polymorpha. Science of Total

450   Environment 444, 43-50.

451   Pedrouzo, M., Borrull, F., Pocurull, E., Marcè, R.M., 2011. Drugs of abuse and their metabolites in

452   waste and surface waters by liquid chromatography-tandem mass spectrometry. Journal of

453   Separation Science 34, 1091-1101.

454   Postigo, C., Lopez de Alda, M.J., Barcelo, D., 2008. Fully automated determination in the low

455   nanogram per litre level of different classes of drugs of abuse in sewage water by on-line solid-

456   phase extraction-liquid chromatography-electrospray-tandem mass spectrometry. Analytical

457   Chemistry 80, 3123-3134.

458   Postigo, C., Lopez de Alma, M.J., Barcelo, D., 2010. Drugs of abuse and their metabolites in the

459   Ebro River basin: occurrence in sewage and surface water, sewage treatment plants removal

460   efficiency, and collective drug usage estimation. Environment International 36, 75-84.

461   Reis, N.M., Li Puma, G., 2015. Novel microfluidics approach for extremely fast and efficient

462   photochemical transformations in fluoropolymer microcapillary films, Chem. Commun. 51 (40),

463   8414-8417.

464 Postigo, C., Sirtori, C., Oller, I., Malato, X., Ignacio Maldonado, M., Lopez de Alda, M., Barcelo,

465 D., 2011. Solar transformation and photocatalytic treatment of cocaine in water: kinetics,

466 characterization of major intermediate products and toxicity evaluation. Applied Catalysis B:

467 Environmental 104, 37-48.

468 Repice, C., Dal Grande, M., Maggi, R., Pedrazzani, R., 2013. Licit and illicit drugs in a wastewater

469 treatment plant in Verona, Italy. Science of the Total Environment 463−464, 27-34.

470 Richardson, S.D., Ternes, T.A., 2014. Water analysis: Emerging contaminants and current issues.

471 Analytical Chemistry 86, 2813−2848.

472 Richardson, S.D., 2012. Environmental Mass Spectrometry: Emerging Contaminants and current

473 issues. Analytical Chemistry 84, 747−778.

474 Russo, D., Spasiano, D., Vaccaro, M., Andreozzi, R., Li Puma, G., Reis, N.M., Marotta, R., 2016.

475 Direct photolysis of benzoylecgonine under UV irradiation at 254 nm in a continuous flow

476 microcapillary film (MCF) array photoreactor. Chemical Engineering Journal 283, 243-250.

477 Terzic, S., Senta, I., Ahel, M., 2010. Illicit drugs in wastewater of the city of Zagreb (Croatia) −

478 estimation of drug abuse in a transition country. Environmental Pollution 158, 2686−2693.

479 Valcarcel, Y., Martinez, F., Gonzalez-Alonso, S., Segura, Y., Català, M., Molina, R., Montero-

480 Rubio, J.C., Mastroianni, N., Lopez de Alma, M., Postigo, C., Barcelò, D., 2012. Drugs of abuse in

481 surface and tap waters of the Tagus River basin: heterogeneous photo-Fenton is effective in their

482 degradation. Environment International 41, 35−43.

483 Van Nuijs, A.L.N., Pecceu, B., Theunis, L., Dubois, N., Charlier, C., Jorens, P.G., Bervoets, L.,

484 Blust, R., Neels, H., Covaci, A., 2009. Cocaine and metabolites in waste and surface water across

485 Belgium. Environmental Pollution 157, 123-129.

486 Van Nuijs, A.L.N., Castiglioni, S., Tarcomnicu, I., Postigo, C., Lopez de Alda, M., Neels, H.,

487 Zuccato, E., Barcelo, D., Covaci, A., 2011. Illicit drug consumption estimations derived from

488 wastewater analysis: a critical review. Science of the Total Environment 409, 3564−3577.

489 Van Nuijs, A.L.N., Abdellati, K., Bervoets, L., Blust, R., Jorens, P.G., Neels, H., Covaci, A., 2012.

490 The stability of illicit drugs and metabolites in wastewater, an important issue for sewage

491 epidemiology?. Journal of Hazardous Materials 239-240, 19−23.

492 Vazquez-Roig, P., Andreu, V., Blasco, C., Pico, Y., 2010. SPE and LC-MS/MS determination of 14

493 illicit drugs in surface waters from the Natural Park of L'Albufera (Valencia, Spain). Analytical and

494 Bioanalytical Chemistry 397, 2851−2864.

495 Wendel, F.M., Luetke Eversloh, C., Machek, E.J., Duirk, S.E., Plewa, M.J., Richardson, S.D.,

496 Ternes, T.A., 2014. Transformation of iopamidol during chlorination. Environmental Science &

497 Technology 48, 12689-12697.

498 World Drug Report, 2012. United Nations Office on Drugs and Crime. Vienna 1-112.

499 Yin Lai, F., Bruno, R., Leung, H.W., Thai, P.K., Ort, C., Carter, S., Thompson, K., Lam, P.K.S.,

500 Mueller, J.F., 2013. Estimating daily and diurnal variations of illicit drug use in Hong Kong: a pilot

501 study of using wastewater analysis in an Asian metropolitan city. Forensic Science International

502 233, 126−132.

503 Zaviska, F., Droqui, P., El Hachemi, E.M., Naffrechoux, E., 2014. Effect of nitrate ions on the

504 efficiency of sonophotochemical phenol degradation. Ultrasonics Sonochemistry 21, 69−75.

505 Zuccato, E., Chiarabrando, C., Castiglioni, S., Calamari, D., Bagnati, R., Schiarea, S., Fanelli, R.,

506 2005. Cocaine in surface water: a new evidence-based tool to monitor community drug abuse.

507 Environmental Health 4, 14.

508 Zuccato, E., Castiglioni, S., Bagnati, R., Chiarabrando, C., Grassi, P., Fanelli, R., 2008. Illicit drugs,

509 a novel group of environmental contaminants. Water Research 42, 961−968.

510 Zuccato, E., Castiglioni, S., 2009. Illicit drugs in the environment. Philosophical Transactions of the

511 Royal Society A 367.

Water matrix	pH	Conductivity (μS)	TOC (ppm)	Nitrates (mg/L)	Nitrites (mg/L)
MilliQ	6.0	2.5	0.248	1.0	**0**
SWW	6.0	80	20.79	1.0	**0**
RWW	7.6	960	43.25	52.4	**0,17**
SurW	7.8	930	46.37	25.8	**0,04**

Tab. 1. Measured parameters of different aqueous matrices. MilliQ (milliQ water); SWW (synthetic wastewater); RWW (real wastewater); SurW (surface water).
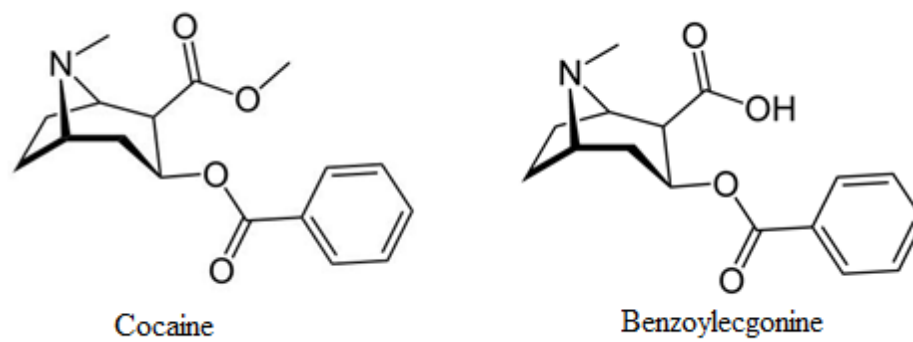
Figure

Fig. 1. Molecular structures of cocaine and benzoylecgonine.

black and white in print is required.
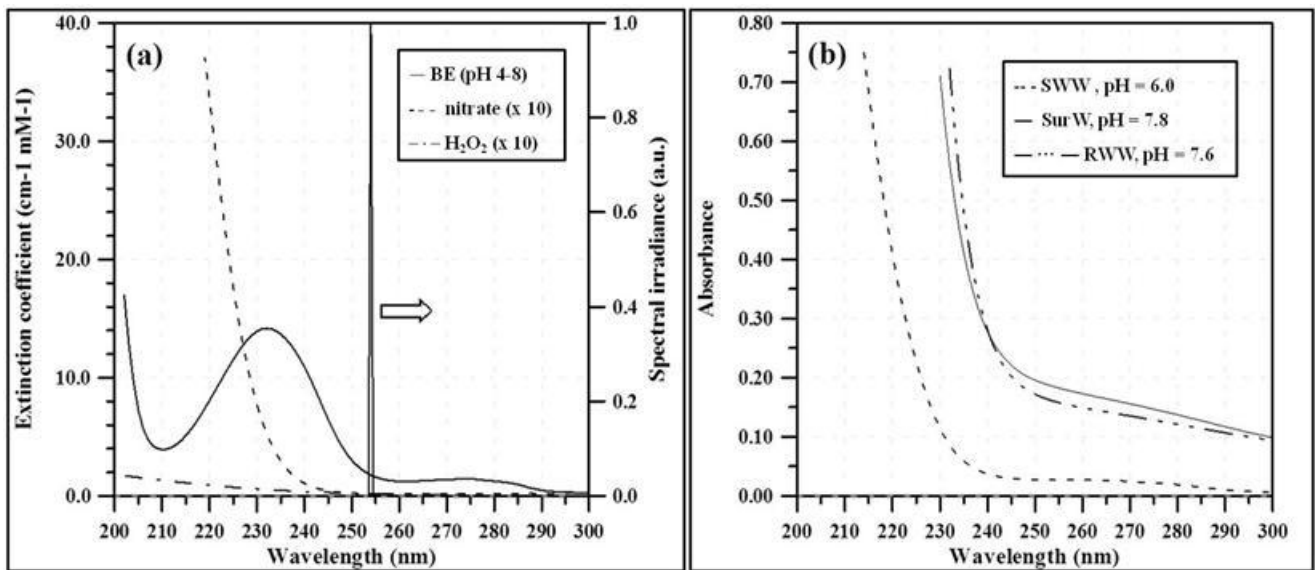
Fig. 2.

Fig. 2a. Extinction coefficient of BE, nitrate and hydrogen peroxide in milliQ water and spectra irradiance of the UV$_{254}$ lamp.

Fig. 2b. Absorbance of the different aqueous matrices.

Black and white in print is required
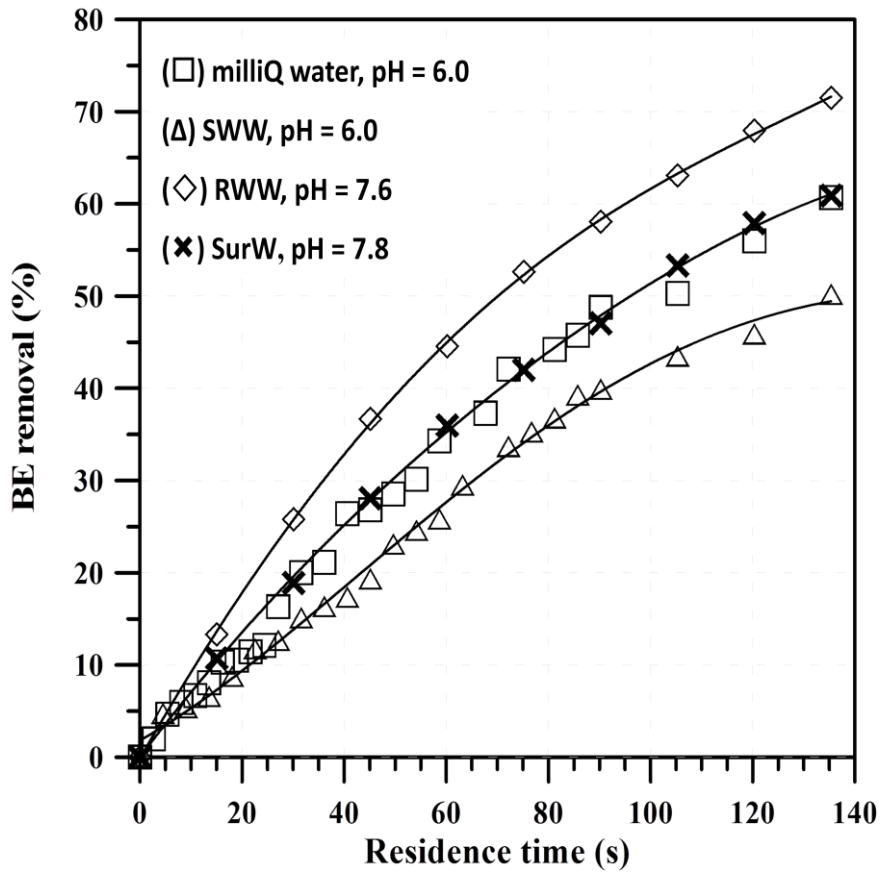
Fig. 3. Removal degree of BE through direct photolysis process. Effect of aqueous matrix. SWW (Synthetic Waste Water) – RWW (Real Waste Water) – SurW (Surface Water). (MilliQ Water, pH = 6.0, data from Russo et al., 2015).

Black and white in print is required.
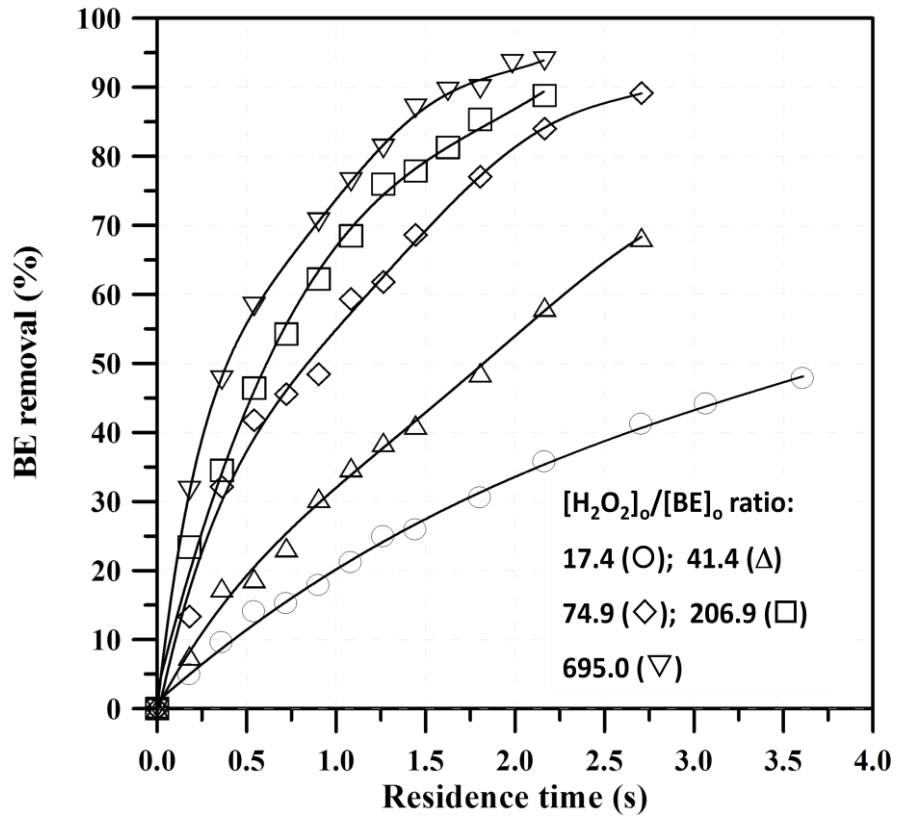
Fig. 4. Removal degree of BE through UV_{254}/H_2O_2 process in milliQ water: effect of $[H_2O_2]_o/[BE]_o$

ratio at pH = 6.0.

Black and white in print is required.
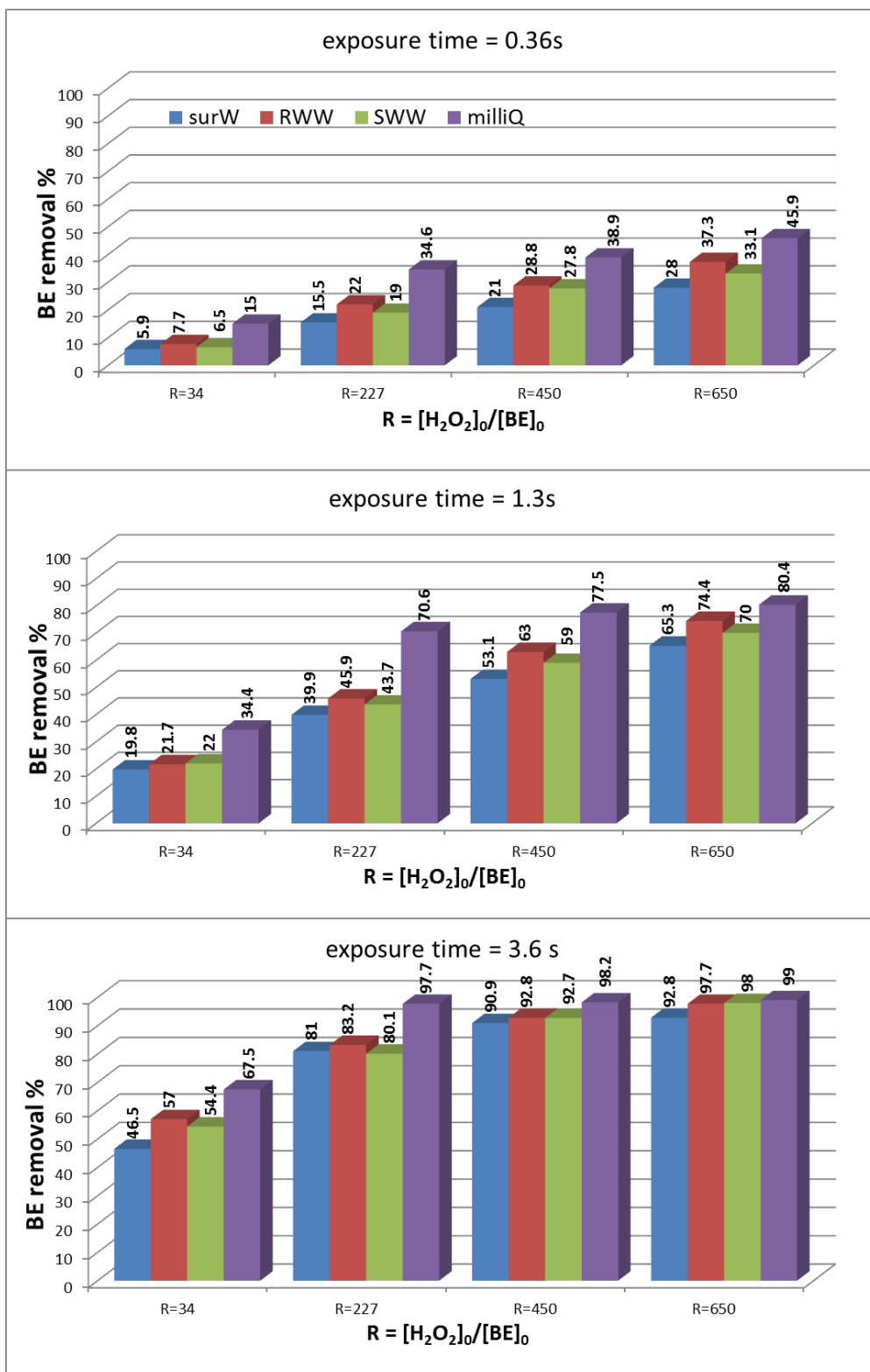
Fig. 5. BE removal degree in different aqueous matrices at various [H₂O₂]ₒ/[BE]ₒ ratios and contact time during UV/H₂O₂ treatment.

Color in print is required.

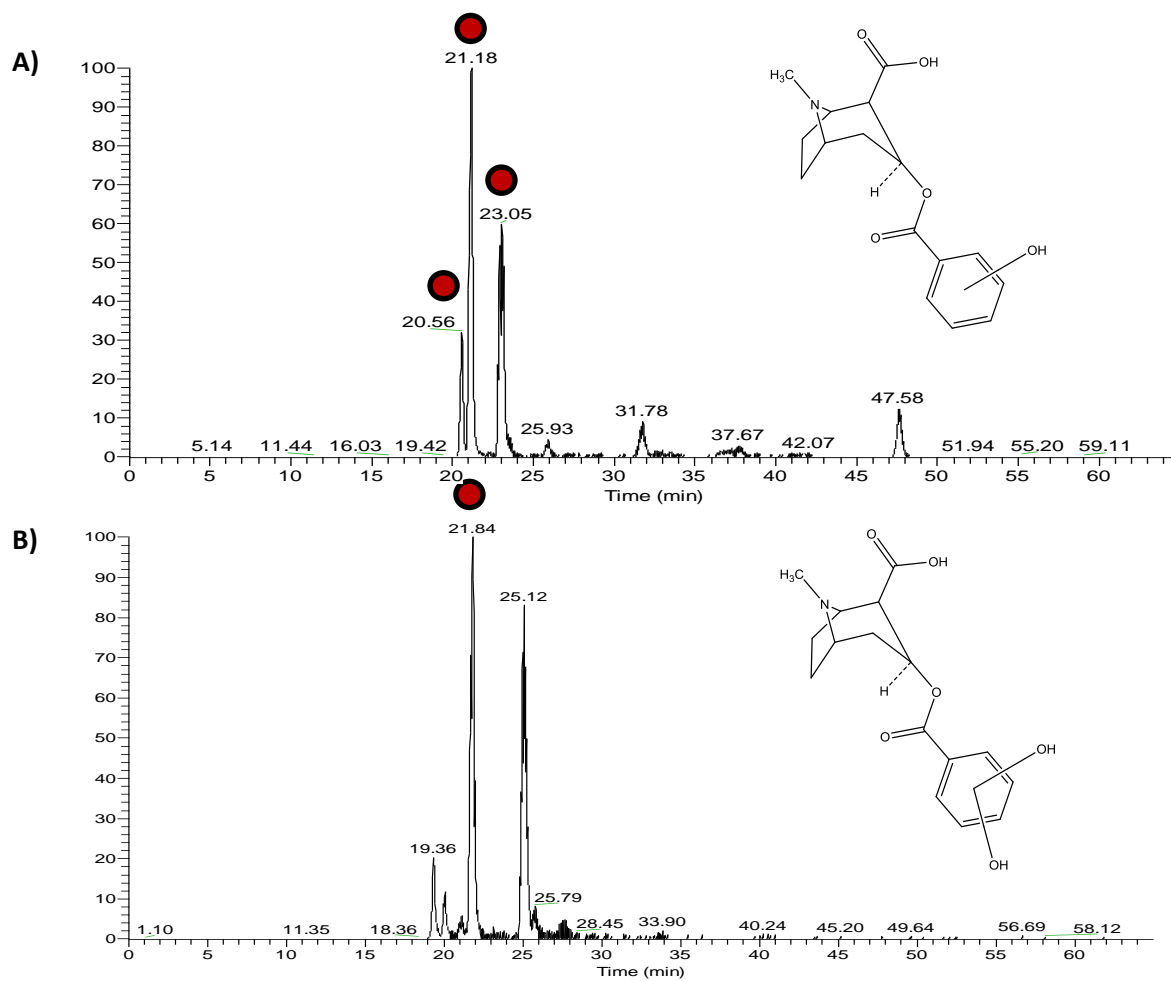**Fig. 6. Extracted ion LC-MS chromatograms for: A) TP 305a, TP 305b, and TP 305c; and B) TP 321, resulting from UV/H₂O₂ reactions with BE (~ 0.5 s reaction time, 40% degradation of BE).**
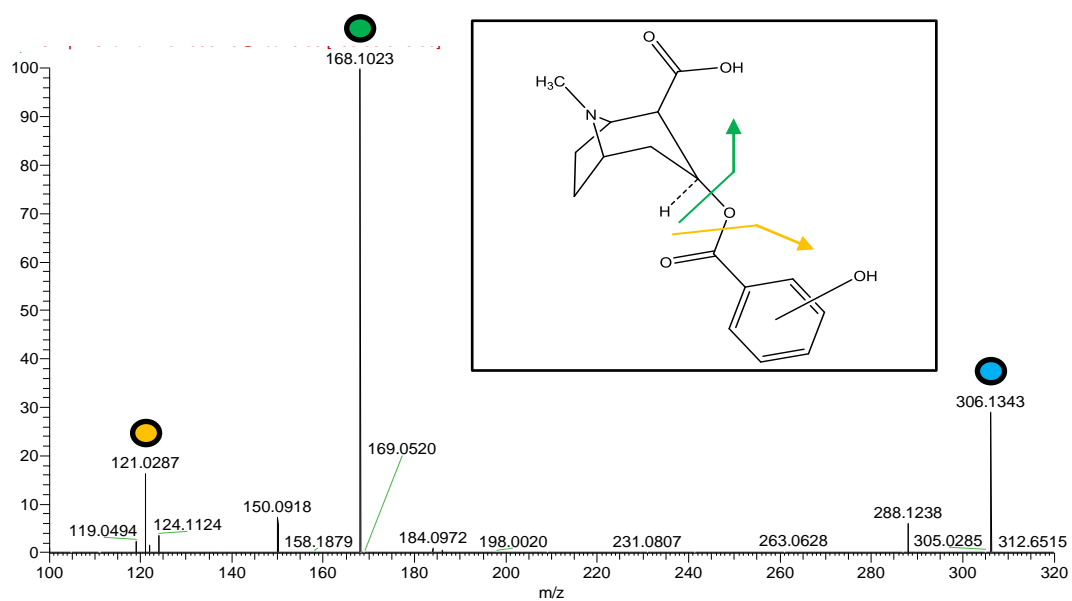
Color in print is required

Fig. 7. Product ion MS/MS spectrum of *m/z* 306.1343 ((M+H)⁺ ion of TP 305) with proposed fragmentation sites.

Color in print is required.

Supplementary data (figure and tables)